PHOTONICS Research

Femtosecond laser-induced periodic surface structures on lithium niobate crystal benefiting from sample heating

Qiang Li,[1] Qiang Wu,[1,2,*] Yanan Li,[1] Chunling Zhang,[1] Zixi Jia,[1] Jianghong Yao,[1,3] Jun Sun,[1,2] and Jingjun Xu[1,2]

[1]Key Laboratory of Weak-Light Nonlinear Photonics, Ministry of Education, TEDA Institute of Applied Physics and School of Physics, Nankai University, Tianjin 300457, China
[2]Collaborative Innovation Center of Extreme Optics, Shanxi University, Taiyuan 030006, China
[3]e-mail: yaojh@nankai.edu.cn
*Corresponding author: wuqiang@nankai.edu.cn

Received 7 February 2018; revised 4 June 2018; accepted 5 June 2018; posted 7 June 2018 (Doc. ID 322686); published 10 July 2018

Periodic surface structures were fabricated by irradiating lithium niobate (LN) crystals with femtosecond laser pulses at sample temperatures ranging from 28°C to 800°C. Carrier density and conductivity of the samples were increased via heating LN, which inhibited coulomb explosion to obtain a uniform periodic surface structure. The periodic surface structures cover an area of 8 mm × 8 mm and have an average spacing of 174 ± 5 nm. Meanwhile, the absorption of the processed sample is about 70% in the spectral range of 400–1000 nm, which is one order of magnitude higher than that of pure LN. Fabrication of periodic surface structures on heating LN with femtosecond laser pulses provides a possibility to generate nanogratings or nanostructures on wide-bandgap transparent crystals.

OCIS codes: (320.7120) Ultrafast phenomena; (160.3730) Lithium niobate; (350.3390) Laser materials processing.

https://doi.org/10.1364/PRJ.6.000789

1. INTRODUCTION

A femtosecond (fs) laser with peak power in the range of gigawatts has been proven to be an efficient tool for precise machining of a wide range of materials, including metals [1], semiconductors [2], polymers [3], and dielectrics (for example, fused silica [4], lithium niobate (LN) [5]). When interacting with a substrate material, the ultrashort pulses ($\sim 10^{-15}$ s) cause minimal thermal diffusion and, therefore, produce more precisely machined features with minimal heat-affected zones [6]. Nonlinear absorption of ultrashort pulse laser energy enables precise manufacturing of hard and brittle materials, such as silica glass [7] or LN crystals [8], which is a challenging task for conventional mechanical manufacturing methods. LN is a multifunctional optoelectronic material with excellent optical and electrical properties, such as the electro-optic effect, acousto-optic effect, pyroelectric effect, piezoelectric effect, photorefractive effect, and nonlinear effect [9–12]. Most devices used in photonic integrated circuits (PICs) [13] can be prepared with an LN crystal, such as an optical waveguide, optical switch, electro-optical modulator, and pyroelectric sensor [14,15]. Achieving a consistent periodic surface microstructure on LN is an important manufacturing step. However, there are still some problems when using a fs laser to prepare micro/nanostructures on the LN crystal's surface. Because of the coulomb explosion, only craters with some stripes at their edge or bottom and groove structures [16,17] on the LN crystal's surface can be obtained, which causes an unstable state of the material surface. These problems will lead that periodic micro/nanostructure on wide-bandgap transparent crystals to not be processed, which influences the process of micro/nano photonic devices, including communication and detecting, as well as biomedical microfluid applications.

In this paper, we report on the application of a heater to control the temperature of LN crystals, which is designed to inhibit the coulomb explosion to obtain a uniform fs laser-induced periodic surface structure (LIPSS). At the same time, we also studied the effect of laser fluence on the sample morphology. The absorption of a processed sample is one order higher than that of pure LN over the wavelength range 400–1000 nm. This approach is beneficial for fabrication of micro/nanostructures on wide-bandgap crystals, which can be used for fabricating nanogratings with antireflection coatings and miniaturized pyroelectric detectors with nanostructures of PICs.

2. EXPERIMENTAL SECTION

The samples were Z-cut LN crystal wafers with an area of 10 mm × 10 mm and a thickness of 500 μm, and the surfaces were optically polished. Each wafer was cleaned with acetone and rinsed in ethanol. The sample was mounted on a three-axis translation stage controlled by a computer in a vacuum chamber, and the laser–matter interaction zone can be observed from different orthogonal directions. The crystal optic axis was aligned parallel to the incident beam and perpendicular to the polarization direction of laser. A heating device was installed in the vacuum chamber to control the temperature of the sample. The sample was processed by a fs laser with a scan speed of 2 mm/s in 500 Torr (1 Torr = 133.322 Pa) N_2. The experimental configuration is shown in Fig. 1. The laser system, consisting of a Ti:sapphire oscillator and a chirped-pulse-regenerative amplifier, produces a 1 kHz train of 120 fs, 1 mJ pulses at 800 nm. An optical shutter in the incident beam path was used to control the pulse numbers. The laser pulses were focused by a lens with a focal length of 50 cm, incident normal to the sample. The spatial profile of the laser pulse was nearly Gaussian with a laser spot radius of 87 μm on the sample surface. A half-wave plate (HWP) and a Glan–Taylor polarizer (GTP) were used to continuously vary the incident energy. The polarization of the laser pulse was controlled by the GTP. Each spot on the sample surface was exposed to 80 laser pulses. After irradiation, the sample was analyzed with a scanning electron microscope (SEM) and a U-4100 spectrophotometer.

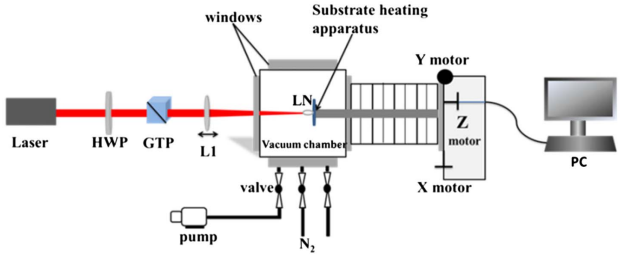

Fig. 1. Schematic illustration of the experimental setup. HWP, half-wave plate; GTP, Glan–Taylor polarizer; L1, convex lens of focal length 50 cm; LN, lithium niobate; PC, personal computer.

3. RESULTS AND DISSCUSION

To evaluate how the elevated sample temperature affects the formation of LIPSS on LN, the experiments were conducted with laser fluence of 7.0 kJ/m^2 and a temperature ranging from 28 to 800°C in steps of 100°C using a carborundum heating plate and two calibrated thermocouples. The morphologies of the samples induced by fs laser under various temperatures are exhibited in Fig. 2. In Fig. 2(a), the crater and groove structures on LN were induced by a fs laser when the temperature of LN was set at 28°C. Researchers believed that such structures were fabricated due to coulomb explosion when a fs laser interacted with dielectrics [18–21]. During the laser irradiating samples, most incident laser energy is absorbed by the electron in its absorption depth. Meanwhile, electrons will escape from the LN surface to form holes (positive charge carriers). This process can be continuously carried out, and the number of holes increased rapidly. The positive charges of the surface are redistributed due to the internal charges' variety of the crystal, and they made the coulomb repulsive force stronger between the internal positive charges, which lead to the coulomb explosion [22,23]. The coulomb explosion causes an unstable state of material surface, so the periodic surface structure cannot be fabricated on LN.

As shown in Fig. 2, the surface structures on LN gradually became more uniform when the temperature increased from 28°C to 800°C. As we know, the main mechanism of electron excitation in LN is through indirect band gap transition [24]. In this process, the optical absorption property of LN highly depends on the number of acoustic phonons, which is a function of temperature [25]. At elevated temperatures, there are

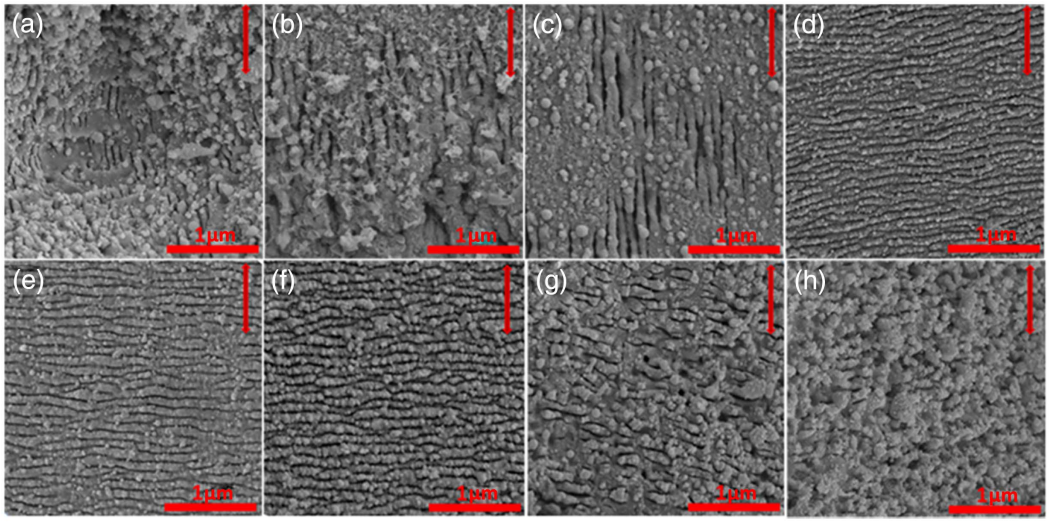

Fig. 2. SEM images of a fs laser processed LN surface in N_2 environment with sample temperature of (a) 28°C, (b) 100°C, (c) 200°C, (d) 300°C, (e) 400°C, (f) 500°C, (g) 600°C, and (h) 800°C, respectively. Fluence, 7.0 kJ/m^2; N_2 pressure, 500 Torr; scanning speed, 2 mm/s. The red double arrow indicates the direction of polarization of the incident laser.

more acoustic phonons, so the electrons have a higher probability to simultaneously absorb acoustic phonons and photons to create the indirect transition. Therefore, a large number of electrons will be photo-excited from the valence band into the conduction band, so more holes would be filled with the electrons from the conduction band. In addition, it has been extensively studied that the conductivity of LN crystals increases with the raising temperature [26,27]. Those will lead to a redistribution of charges in the crystal to form a new equilibrium state; hence, the coulomb repulsion force will be reduced, and the coulomb explosion will be inhibited [28]. At the same time, LIPSS results from the competition between periodic surface structuring originating from the interference of incident light with surface plasmon polaritons (SPPs) and surface smoothing associated with surface melting and softening [29]. Researchers believed that the stimulation of periodic surface structuring by SPPs is, hence, crucial for the evolvement of fs-LIPSS [30–34], while surface melting produces smoothing and, hence, plays a counteracting role in preventing fs-LIPSS formation.

In addition, Fig. 2 shows that the integrated periodic surface structures on LN cannot be formed below 300°C, and the direction of formed ripples is parallel to the laser polarization direction. However, when the temperature is raised to 300°C, the periodic surface structures change into comparatively uniform ripples, and their direction is perpendicular to the laser polarization direction. We propose that the reason for the changes of periodic surface structures and direction is that the optical absorption of LN at 800 nm of wavelength has a precipitous increase around 300°C when temperature increases [35].

The optical properties of LN were influenced by LIPSS. A U-4100 spectrophotometer was used to measure the absorption spectra of LNs processed by a fs laser under different temperatures. As shown in Fig. 3, the processed LNs display strong absorption from visible to near-IR range. The absorption spectra depend on the surface structures under different temperature conditions. The absorption of pure LN is approximately 5% in the spectral range of 400–1000 nm due to the defect absorption, while Fig. 3(a) indicates that the absorption of LN with fs-LIPSS is up to 70%, which is one order of magnitude higher than that of pure LN. As seen from Figs. 3(a) and 3(b), the absorption of processed LN at sample temperature from 28°C to 800°C has been significantly increased.

As seen from Fig. 2, the surface structures on LN become more uniform when the temperature increased from 28°C to 500°C. The light-trapping effect of the samples will be better, which will directly lead to the absorption increasing. Therefore, the absorption of samples will increase with the improvement of surface structure. When the temperature was raised to 500°C, the surface structure of LN was damaged due to the micro-explosion during fs laser processing. So, there is a significant decrease trend in absorption when the temperature exceeds 500°C.

During the processing procedure by the fs laser, the pulse fluence can affect the surface morphology as well as LN temperature. Therefore, experiments of machining LN were conducted under different laser fluences when the sample

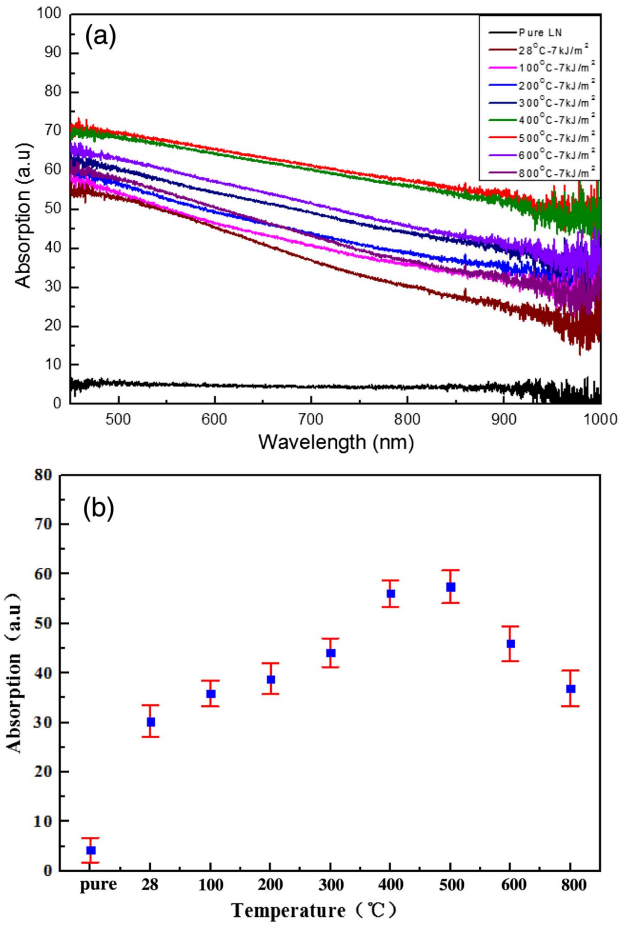

Fig. 3. (a) Absorption spectra of fs laser processed LN; (b) absorption at 800 nm dependence of LN processed under the different temperatures. All samples were fabricated with the fluence of 7.0 kJ/m^2 at 2 mm/s scanning speed, 500 Torr N_2 pressure, and the temperatures of 28°C, 100°C, 200°C, 300°C, 400°C, 500°C, 600°C, and 800°C, respectively.

temperatures were raised up to near the suitable temperature (500°C). Figure 4 shows SEM images of LN irradiated by a fs laser with fluence of 5.0, 6.0, 7.0, and 8.0 kJ/m^2, respectively. The sample shown in Fig. 4(a) was fabricated under 5.0 kJ/m^2 (slightly higher than the ablation threshold), which only had some shallow and discontinuous surface structures with small roughness. The fluence irradiating samples shown in Fig. 4(b) were somewhat lower than the suitable fluence, and the treated area appears in the discontinuous and uniform surface structure. The sample of Fig. 4(c) was fabricated under 7.0 kJ/m^2 of suitable fluence, and the ablated area was covered with continuous uniform LIPSS. The period Λ of LIPSS was approximately 174 ± 5 nm, and its orientations were perpendicular to the laser polarization. However, when the fluence was far higher than the suitable fluence, the coulomb explosion of material occurred, the ablated surface became a bumpy surface, and the roughness is large in the micron scale [see the area of Fig. 4(d)]. These results implied that laser fluence played a key role for the morphology and quality of the formed LIPPS when the sample temperature was in an appropriate range.

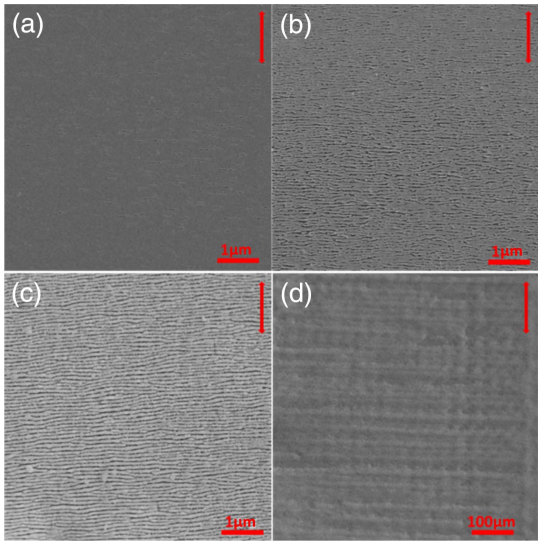

Fig. 4. SEM images of the periodic surface structures formed by the irradiation of a linearly polarized laser under the sample temperature of 500°C. Fluences: (a) 5.0, (b) 6.0, (c) 7.0, (d) 8.0 kJ/m^2, respectively. The red double arrow indicates the direction of polarization of the incident laser.

4. CONCLUSION

In conclusion, our results demonstrate that periodic structures can be fabricated on an LN surface by fs laser irradiation under proper sample temperatures and appropriate laser fluence. The carrier density and conductivity of the samples are increased via heating the samples, which inhibits coulomb explosion and thus leads to a uniform fs-LIPSS. The formed periodic surface structures on LN give rise to enhanced absorption efficiency from the visible to near-IR range. The processed LN, which is covered with large area periodic surface structures, has broad potential applications in new miniaturized photoelectric devices and nanograting for antireflection coating. This technique is considerably valuable for manufacturing structures on wide-bandgap transparent crystals with a fs laser. For example, it can inhibit the rough boundary, burr, and chipping in hole drilling, waveguide machining, and crystal cutting, which are induced by the coulomb explosion.

Funding. National Natural Science Foundation of China (NSFC) (11574158, 61378018); 111 Project (B07013); Program for Changjiang Scholars and Innovative Research Team in University (IRT_13R29); Fundamental Research Funds for the Central Universities.

REFERENCES

1. K. Furusawa, K. Takahashi, H. Kumagai, K. Midorikawa, and M. Obara, "Ablation characteristics of Au, Ag, and Cu metals using a femtosecond Ti:sapphire laser," Appl. Phys. A **69**, S359–S366 (1999).
2. T.-H. Her, R. J. Finlay, C. Wu, and E. Mazur, "Femtosecond laser-induced formation of spikes on silicon," Appl. Phys. A **70**, 383–385 (2000).
3. H. Kumagai, K. Midorikawa, K. Toyoda, S. Nakamura, T. Okamoto, and M. Obara, "Ablation of polymer films by a femtosecond high-peak-power Ti:sapphire laser at 798 nm," Appl. Phys. Lett. **65**, 1850–1852 (1994).
4. Y. Dai, G. Wu, X. Lin, G. Ma, and J. Qiu, "Femtosecond laser induced rotated 3D self-organized nanograting in fused silica," Opt. Express **20**, 18072–18078 (2012).
5. R. R. Gattass and E. Mazur, "Femtosecond laser micromachining in transparent materials," Nat. Photonics **2**, 219–225 (2008).
6. M. Halbwax, T. Sarnet, P. Delaporte, M. Sentis, H. Etienne, F. Torregrosa, V. Vervisch, I. Perichaud, and S. Martinuzzi, "Micro and nano-structuration of silicon by femtosecond laser: application to silicon photovoltaic cells fabrication," Thin Solid Films **516**, 6791–6795 (2008).
7. Q. Sun, F. Liang, R. Vallée, and S. L. Chin, "Nanograting formation on the surface of silica glass by scanning focused femtosecond laser pulses," Opt. Lett. **33**, 2713–2715 (2008).
8. G. A. Torchia, C. Mendez, and D. Jaque, "Laser gain in femtosecond microstructured Nd:MgO:$LiNbO_3$ crystals," Appl. Phys. B **83**, 559–563 (2006).
9. A. Bouchier, G. Lucas-Leclin, and P. Georges, "Frequency doubling of an efficient continuous wave single-mode Yb-doped fiber laser at 978 nm in a periodically-poled MgO:$LiNbO_3$ waveguide," Opt. Express **13**, 6974–6979 (2005).
10. Y. Kong, S. Liu, Y. Zhao, H. Liu, S. Chen, and J. Xu, "Highly optical damage resistant crystal: zirconium-oxide-doped lithium niobate," Appl. Phys. Lett. **91**, 081908 (2007).
11. L. Razzari, P. Minzioni, and I. Cristiani, "Photorefractivity of Hafnium-doped congruent lithium-niobate crystals," Appl. Phys. Lett. **86**, 131914 (2005).
12. R. S. Weis and T. K. Gaylord, "Lithium niobate: summary of physical properties and crystal structure," Appl. Phys. A **37**, 191–203 (1985).
13. P. Wang, J. Qi, Z. Liu, Y. Liao, W. Chu, and Y. Cheng, "Fabrication of polarization-independent waveguides deeply buried in lithium niobate crystal using aberration-corrected femtosecond laser direct writing," Sci. Rep. **7**, 41211–41217 (2017).
14. S. Kroesen, W. Horn, J. Imbrock, and C. Denz, "Electro-optical tunable waveguide embedded multiscan Bragg gratings in lithium niobate by direct femtosecond laser writing," Opt. Express **22**, 23339–23348 (2014).
15. F. Chen, "Photonic guiding structures in lithium niobate crystals produced by energetic ion beams," J. Appl. Phys. **106**, 081101 (2009).
16. B. Yu, P. Lu, N. Dai, Y. Li, X. Wang, Y. Wang, and Q. Zheng, "Femtosecond laser-induced sub-wavelength modification in lithium niobate single crystal," J. Opt. A **10**, 035301 (2008).
17. H. Shimizu, G. Obara, M. Terakawa, E. Mazur, and M. Obara, "Evolution of femtosecond laser-induced surface ripples on lithium niobate crystal surfaces," Appl. Phys. Express **6**, 112701 (2013).
18. J. Bonse, J. Krüger, S. Höhm, and A. Rosenfeld, "Femtosecond laser-induced periodic surface structures," J. Laser Appl. **24**, 042006 (2012).
19. D. Tan, K. N. Sharafudeen, Y. Z. Yue, and J. R. Qiu, "Femtosecond laser induced phenomena in transparent solid materials: fundamentals and applications," Prog. Mater. Sci. **76**, 154–228 (2016).
20. R. Stoian, D. Ashkenasi, A. Rosenfeld, and E. E. B. Campbell, "Coulomb explosion in ultrashort pulsed laser ablation of Al_2O_3," Phys. Rev. B **62**, 13167–13173 (2000).
21. N. M. Bulgakova, R. Stoian, A. Rosenfeld, I. V. Hertel, W. Marine, and E. E. B. Campbell, "A general continuum approach to describe fast electronic transport in pulsed laser irradiated materials: the problem of Coulomb explosion," Appl. Phys. A **81**, 345–356 (2005).
22. J. Reif, F. Costache, M. Henyk, and S. V. Pandelov, "Ripples revisited: non-classical morphology at the bottom of femtosecond laser ablation craters in transparent dielectrics," Appl. Surf. Sci. **197**, 891–895 (2002).
23. B. C. Stuart, M. D. Feit, S. Herman, A. M. Rubenchik, B. W. Shore, and M. D. Perry, "Nanosecond-to-femtosecond laser-induced breakdown in dielectrics," Phys. Rev. B **53**, 1749–1761 (1996).
24. J. Reif, "Processing with ultrashort laser pulses," in *Laser Processing of Materials: Fundamentals, Applications and Developments*, R. M. Osgood, ed. (Springer, 2010), Chap. 6.
25. M. Y. Shen, C. H. Crouch, J. E. Carey, R. Younkin, E. Mazur, M. Sheehy, and C. M. Friend, "Formation of regular arrays of silicon

microspikes by femtosecond laser irradiation through a mask," Appl. Phys. Lett. **82**, 1715–1717 (2003).
26. L. Kovacs and K. Polgar, "Electrical and pyroelectric properties," in *Properties of Lithium Niobate*, K. K. Wong, ed. (Inspec, 2002), Chap. 6.
27. S. A. Basun, G. Cook, and D. R. Evans, "Direct temperature dependence measurements of dark conductivity and two-beam coupling in $LiNbO_3$:Fe," Opt. Express **16**, 3993–4000 (2008).
28. A. J. Eccles, J. A. van den Berg, A. Brown, and J. C. Vickerman, "Evidence of a charge induced contribution to the sputtering yield of insulating and semiconducting materials," Appl. Phys. Lett. **49**, 188–190 (1986).
29. M. Yang, Q. Wu, Z. Chen, B. Zhang, B. Tang, J. Yao, I. D. Olenik, and J. Xu, "Generation and erasure of femtosecond laser-induced periodic surface structures on nanoparticle-covered silicon by a single laser pulse," Opt. Lett. **39**, 343–346 (2014).
30. J. Bonse, A. Rosenfeld, and J. Krüger, "On the role of surface plasmon polaritons in the formation of laser-induced periodic surface structures upon irradiation of silicon by femtosecond-laser pulses," J. Appl. Phys. **106**, 104910 (2009).
31. J. Reif, O. Varlamova, S. Varlamov, and M. Bestehorn, "The role of asymmetric excitation in self-organized nanostructure formation upon femtosecond laser ablation," AIP Conf. Proc. **1464**, 428–441 (2012).
32. J. Reif, O. Varlamova, and F. Costache, "Femtosecond laser induced nanostructure formation: self-organization control parameters," Appl. Phys. A **92**, 1019–1024 (2008).
33. M. Huang, F. Zhao, Y. Cheng, N. Xu, and Z. Xu, "Origin of laser-induced near-subwavelength ripples: interference between surface plasmons and incident laser," ACS Nano **3**, 4062–4070 (2009).
34. T.-H. Her, R. J. Finlay, C. Wu, S. Deliwala, and E. Mazur, "Microstructuring of silicon with femtosecond laser pulses," Appl. Phys. Lett. **73**, 1673–1675 (1998).
35. J. Koppitz, O. F. Schirmer, and A. I. Kuznetsov, "Thermal dissociation of bipolarons in reduced undoped $LiNbO_3$," Europhys. Lett. **4**, 1055–1059 (1987).